Int. J. Therm. Sci. (2001) 40, 528–538

S1290-0729(01)01241-8/FLA

Inverse radiation problem of source term in three-dimensional complicated geometric semitransparent media

Lin-Hua Liu *, He-Ping Tan, Zhi-Hong He

School of Energy Science and Engineering, Harbin Institute of Technology, 92 West Dazhi Street, Harbin 150001, PR China

(Received 11 May 2000, accepted 23 August 2000)

Abstract — A method is presented to identify the three-dimensional source term distribution in complicated geometric systems of known radiative properties from the knowledge of the radiative intensities exiting the boundaries. The inverse radiation problem is formulated as an optimization problem, and solved by the conjugate gradient method that minimizes the errors between the exit radiative intensities calculated and the experimental measurements. The analysis consists of the direct problem, the gradient equation, and the sensitivity problem. In this approach, the discrete ordinates method is employed to solve the direct and the sensitivity problems in general body-fitted coordinates. The effects of the measurement errors on the accuracy of the inverse analysis are investigated. The study shows that the three-dimensional source term distribution in complicated geometric systems can be estimated accurately, even with noisy data. © 2001 Éditions scientifiques et médicales Elsevier SAS

radiative heat transfer / inverse problem / source term / semitransparent media / complicated geometric system

Nomenclature

c_{ijk}	expansion coefficients for temperature distribution function	
$\boldsymbol{c}$	$= [c_{000}, c_{100}, \ldots, c_{\mathrm{QRS}}]^{\mathrm{T}}$	
$\boldsymbol{d}$	direction of descent	
g	scattering asymmetry parameter	
I	radiation intensity	$\mathrm{W{\cdot}m^{-2}{\cdot}sr^{-1}}$
∇I	sensitivity coefficient vector	
J	Jacobian	
M	total number of the discrete ordinates	
N	number of sensors	
$\boldsymbol{n}$	surface normal vector	
$\overline{n}$	refractive index	
S	source term	$\mathrm{W{\cdot}m^{-2}{\cdot}sr^{-1}}$
$\boldsymbol{s}$	direction vector	
T	temperature	K
w	quadrature weights	
x, y, z	optical coordinates	
Y	measured exit radiative intensity at boundary	$\mathrm{W{\cdot}m^{-2}{\cdot}sr^{-1}}$
α, β, γ	direction cosines	
Γ	objective function	
$\nabla\Gamma$	gradient of the objective function	
δ	measured errors of exit radiative intensity	
ε	a small specified positive number	
ξ, η, ζ	body-fitted coordinates	
ς	random variable	
μ	step size	
ν	conjugate coefficient	
ρ_g	errors of scattering asymmetry parameter	
ρ_ω	errors of single scattering albedo	
σ	standard deviation	
$\overline{\sigma}$	Stefan–Boltzmann constant	
$\boldsymbol{\tau}$	position vector	
Φ	scattering phase function	
ω	single scattering albedo	
Ω	solid angle	

Subscripts

av	average value

Superscripts

k	kth iteration
m	the direction of discrete ordinates
T	matrix inverse

* Correspondence and reprints.
E-mail addresses: tanhp@etp4.hit.edu.cn (L.-H. Liu), tanhp@etp4.hit.edu.cn (H.-T. Tan), tanhp@etp4.hit.edu.cn (Z.-H. He).

1. INTRODUCTION

Inverse radiation analysis is concerned with the determination of the radiation properties, boundary condition, and the temperature profile or source term distribution from various types of radiation measurements. The subject has been extensively reviewed in a series of papers by McCormick [1–4]. A considerable amount of work has been reported for determining the single-scattering albedo, scattering phase function, absorption coefficient, scattering coefficient, boundary condition, or the optical thickness of a medium from various types of radiation measurements [5–16]. Inverse problems that deal with the prediction of the source term or temperature distribution in a medium from radiation measurements have also been reported by many researchers [17–29]. Yi [17], Li and Ozisik [18, 19], Siewert [20–22], Li [23, 24], Liu, Tan and Yu [25–27] have reconstructed the temperature profiles or source terms in one-dimensional plane-parallel, spherical, or cylindrical media by the inverse analysis from the data of the radiation intensities exiting the boundaries. Li [28] has studied the inverse problem of unknown source term in a two-dimensional rectangular medium with transparent boundaries. Liu, Tan and Yu [29] have reconstructed the temperature distribution function in a three-dimensional rectangular medium with gray opaque boundaries. Despite the relatively large interest expressed in inverse radiation problems of temperature or source term distributions in a medium, most of the work has considered one-dimensional problems, and all of the work has been focused on regular geometric systems.

The inverse radiation problem considered in this paper is concerned with estimation of the source term distribution in a three-dimensional complicated geometric system, which contains absorbing, emitting, scattering gray medium, from the knowledge of the radiative intensities exiting boundaries. The radiative properties, such as single scattering albedo and scattering phase function of the medium, are assumed to be uniform everywhere. The boundaries are considered to be transparent. The inverse problem is formulated as an optimization problem and the conjugate gradient method is used for its solution. In this approach, the discrete ordinates method is employed to solve the direct and the sensitivity problems in general body-fitted coordinates. The analysis consists of the direct problem, the gradient equation, and the sensitivity problem. We describe the procedure for each of these steps and then present an algorithm for the solution of the inverse radiation problem. Finally, several three-dimensional inverse problems of source term in the complicated geometric system are investigated to demonstrate the computational accuracy and efficiency of the inverse analysis method presented in this paper.

2. ANALYSIS

2.1. Direct problem

Consider the radiative transfer processes in a three-dimensional gray medium. The boundary surfaces are considered to be transparent. There is no external incident radiation. The radiative properties, such as single scattering albedo ω and scattering phase function $\Phi(\boldsymbol{s}', \boldsymbol{s})$ of the medium, are assumed to be uniform everywhere. The direct problem of concern here is to find the radiative intensities exiting the boundaries for the known source term distribution and radiative properties. The radiative transfer equation can be written in the form [30]

$$\boldsymbol{s} \cdot \nabla I(\boldsymbol{\tau}, \boldsymbol{s}) = -I(\boldsymbol{\tau}, \boldsymbol{s}) + S(\boldsymbol{\tau}) + \frac{\omega}{4\pi} \int_{\Omega'=4\pi} I(\boldsymbol{\tau}, \boldsymbol{s})\, \Phi(\boldsymbol{s}', \boldsymbol{s})\, \mathrm{d}\Omega' \quad (1)$$

with the boundary conditions

$$I(\boldsymbol{\tau}_w, \boldsymbol{s}) = 0, \qquad \boldsymbol{n}_w \cdot \boldsymbol{s} > 0 \quad (2)$$

where $I(\boldsymbol{\tau}, \boldsymbol{s})$ is the radiative intensity, which is a function of position vector $\boldsymbol{\tau}$ and direction $\boldsymbol{s}$; Ω is the solid angle, $\boldsymbol{\tau}_w$ and $\boldsymbol{n}_w$ represent the boundary and the unit normal vector on the boundary, respectively. The source term $S(\boldsymbol{\tau})$ is related to the temperature $T(\boldsymbol{\tau})$ of the medium by

$$S(\boldsymbol{\tau}) = \frac{(1-\omega)\overline{n}^2 \overline{\sigma}\, T^4(\boldsymbol{\tau})}{\pi} \quad (3)$$

Here, $\overline{n}$ is the refractive index and $\overline{\sigma}$ is the Stefan–Boltzmann constant.

We apply the discrete ordinates method (DOM) to solve the direct problem. In the DOM, equations (1) and (2) are replaced by a discrete set of equations for a finite number of ordinate directions. The integral terms on the right-hand side of equation (1) are approximated by summation over each ordinate. In the Cartesian ordinate system, the discrete ordinates equation can be written as [30–33]

$$\alpha^m \frac{\partial I^m}{\partial x} + \beta^m \frac{\partial I^m}{\partial y} + \gamma^m \frac{\partial I^m}{\partial z} = -I^m + S(\boldsymbol{\tau}) + \frac{\omega}{4\pi} \sum_{m'=1}^{M} w^{m'} \Phi^{mm'} I^{m'} \quad (4)$$

with the boundary conditions

$$I^m(\boldsymbol{\tau}_w) = 0, \qquad \boldsymbol{n}_w \cdot \boldsymbol{s}^m > 0 \quad (5)$$

where subscripts m and m' denote the discrete directions; w is the quadrature weight, x, y and z are the optical coordinates, α, β, γ are direction cosines.

For a problem with an irregular geometry, a differential equation in orthogonal Cartesian coordinates such as equation (4) is usually transformed into an equation in general body-fitted coordinates for convenience of solution [34]. This will provide a more accurate prediction of radiative heat transfer, especially on the boundaries, than the blocked-off region treatment for a complicated geometry. Liu et al. [35] have studied five benchmark problems of radiative heat transfer in irregular geometries, and found that the DOM is accurate and efficient in general body-fitted coordinates. The full conservative form of the discrete ordinates equation in a general body-fitted coordinate system (ξ, η, ζ) is obtained from equation (4) as

$$\frac{\partial}{\partial \xi}\left[\left(\alpha^m \xi_x + \beta^m \xi_y + \gamma^m \xi_z\right) J I^m\right] + \frac{\partial}{\partial \eta}\left[\left(\alpha^m \eta_x + \beta^m \eta_y + \gamma^m \eta_z\right) J I^m\right] + \frac{\partial}{\partial \zeta}\left[\left(\alpha^m \zeta_x + \beta^m \zeta_y + \gamma^m \zeta_z\right) J I^m\right] = J\left[-I^m + S(\boldsymbol{\tau}) + \frac{\omega}{4\pi} \sum_{m'=1}^{M} w^{m'} \Phi^{mm'} I^{m'}\right] \quad (6)$$

where J is the Jacobian of the coordinate transformation and is given as

$$J = \begin{vmatrix} \frac{\partial x}{\partial \xi} & \frac{\partial x}{\partial \eta} & \frac{\partial x}{\partial \zeta} \\ \frac{\partial y}{\partial \xi} & \frac{\partial y}{\partial \eta} & \frac{\partial y}{\partial \zeta} \\ \frac{\partial z}{\partial \xi} & \frac{\partial z}{\partial \eta} & \frac{\partial z}{\partial \zeta} \end{vmatrix} \quad (7)$$

Equation (7) is spatially discretized by well-known control-volume technique. For a representative control volume, the spatially discretized discrete ordinates equation in a general body-fitted coordinates is obtained as

$$\begin{aligned} &\left\{\left[\left(\alpha^m \xi_x + \beta^m \xi_y + \gamma^m \xi_z\right) I^m J\right]_{\mathrm{e}} - \left[\left(\alpha^m \xi_x + \beta^m \xi_y + \gamma^m \xi_z\right) I^m J\right]_{\mathrm{w}}\right\} \Delta\eta\Delta\zeta \\ &+ \left\{\left[\left(\alpha^m \eta_x + \beta^m \eta_y + \gamma^m \eta_z\right) I^m J\right]_{\mathrm{n}} - \left[\left(\alpha^m \eta_x + \beta^m \eta_y + \gamma^m \eta_z\right) I^m J\right]_{\mathrm{s}}\right\} \Delta\xi\Delta\eta \\ &+ \left\{\left[\left(\alpha^m \zeta_x + \beta^m \zeta_y + \gamma^m \zeta_z\right) I^m J\right]_{\mathrm{t}} - \left[\left(\alpha^m \zeta_x + \beta^m \zeta_y + \gamma^m \zeta_z\right) I^m J\right]_{\mathrm{b}}\right\} \Delta\xi\Delta\eta \\ &= J_{\mathrm{P}}\left[-I^m + S(\boldsymbol{\tau}) + \frac{\omega}{4\pi} \sum_{m'=1}^{M} w^{m'} \Phi^{mm'} I^{m'}\right]_{\mathrm{P}} \cdot \Delta\xi\Delta\eta\Delta\zeta \end{aligned} \quad (8)$$

Here, the subscripts e, w, etc. indicate that the values inside the brackets have to be taken at the eastern, western, etc. control volume surfaces, respectively; the subscript P represents the value at the central node of the control volume.

To close the above system of equations, relations are needed between the intensities on the control volume surfaces and nodal intensities. In this study, the step scheme [30–33], which sets the downstream surface intensities equal to the upstream nodal intensities, is used. The final discretized equation for equation (6) can be written in the form

$$a_{\mathrm{P}}^m I_{\mathrm{P}}^m = a_{\mathrm{E}}^m I_{\mathrm{E}}^m + a_{\mathrm{W}}^m I_{\mathrm{W}}^m + a_{\mathrm{N}}^m I_{\mathrm{N}}^m + a_{\mathrm{S}}^m I_{\mathrm{S}}^m + a_{\mathrm{T}}^m I_{\mathrm{T}}^m + a_{\mathrm{B}}^m I_{\mathrm{B}}^m + b^m \quad (9)$$

where the intensities with the subscripts E, W, etc. denote the eastern, western, etc. nodal intensities, and

$$a_{\mathrm{E}}^m = \max\left\{-\left[\left(\alpha^m \xi_x + \beta^m \xi_y + \gamma^m \xi_z\right) J\right]_{\mathrm{e}} \Delta\eta\Delta\zeta, 0\right\} \quad (10a)$$

$$a_{\mathrm{W}}^m = \max\left\{\left[\left(\alpha^m \xi_x + \beta^m \xi_y + \gamma^m \xi_z\right) J\right]_{\mathrm{w}} \Delta\eta\Delta\zeta, 0\right\} \quad (10b)$$

$$a_{\mathrm{N}}^m = \max\left\{-\left[\left(\alpha^m \eta_x + \beta^m \eta_y + \gamma^m \eta_z\right) J\right]_{\mathrm{n}} \Delta\xi\Delta\zeta, 0\right\} \quad (10c)$$

$$a_{\mathrm{S}}^m = \max\left\{\left[\left(\alpha^m \eta_x + \beta^m \eta_y + \gamma^m \eta_z\right) J\right]_{\mathrm{s}} \Delta\xi\Delta\zeta, 0\right\} \quad (10d)$$

$$a_{\mathrm{T}}^m = \max\left\{-\left[\left(\alpha^m \zeta_x + \beta^m \zeta_y + \gamma^m \zeta_z\right) J\right]_{\mathrm{t}} \Delta\xi\Delta\eta, 0\right\} \quad (10e)$$

$$a_{\mathrm{B}}^m = \max\left\{\left[\left(\alpha^m \zeta_x + \beta^m \zeta_y + \gamma^m \zeta_z\right) J\right]_{\mathrm{b}} \Delta\xi\Delta\eta, 0\right\} \quad (10f)$$

$$a_{\mathrm{P}}^m = \max\left\{\left[\left(\alpha^m \xi_x + \beta^m \xi_y + \gamma^m \xi_z\right) J\right]_{\mathrm{e}} \Delta\eta\Delta\zeta, 0\right\} + \max\left\{-\left[\left(\alpha^m \zeta_x + \beta^m \zeta_y + \gamma^m \zeta_z\right) J\right]_{\mathrm{w}} \Delta\eta\Delta\zeta, 0\right\}$$

$$+\max\left\{\left[\left(\alpha^m\eta_x+\beta^m\eta_y+\gamma^m\eta_z\right)J\right]_{\mathrm{n}}\Delta\xi\,\Delta\zeta,0\right\}$$
$$+\max\left\{-\left[\left(\alpha^m\eta_x+\beta^m\eta_y+\gamma^m\eta_z\right)J\right]_{\mathrm{s}}\Delta\xi\,\Delta\zeta,0\right\}$$
$$+\max\left\{\left[\left(\alpha^m\zeta_x+\beta^m\zeta_y+\gamma^m\zeta_z\right)J\right]_{\mathrm{t}}\Delta\xi\,\Delta\eta,0\right\}$$
$$+\max\left\{-\left[\left(\alpha^m\zeta_x+\beta^m\zeta_y+\gamma^m\zeta_z\right)J\right]_{\mathrm{b}}\Delta\xi\,\Delta\eta,0\right\}$$
$$+J_{\mathrm{P}}\left[1-\frac{\omega w^m\Phi^{mm}}{4\pi}\right]_{\mathrm{P}}\Delta\xi\,\Delta\eta\,\Delta\zeta \tag{10g}$$

$$b^m=J_{\mathrm{P}}\left[S(\boldsymbol{\tau})+\frac{\omega}{4\pi}\sum_{m'=1,m'\neq m}^{M}w^{m'}\Phi^{mm'}I^{m'}\right]_{\mathrm{P}}\cdot\Delta\xi\,\Delta\eta\,\Delta\zeta \tag{10h}$$

Equation (10) can be rewritten in matrix notation as follows:

$$\boldsymbol{A}\varphi=\boldsymbol{Q} \tag{11}$$

where $\boldsymbol{A}$ is the seven-diagonal non-symmetric coefficient matrix, φ is a vector containing the variable values I^m at grid nodes, and $\boldsymbol{Q}$ is the vector containing the terms b^m on the right-hand side of equation (9). The preceding spatial discretization of equation (6) is carried in one discrete direction. The same discretization procedure is applied to all discrete directions. This forms systems of nonsymmetric algebraic equations. Each direction is solved independently. Recently, there are many methods for solving linear algebraic equations, for example, CGS (conjugate gradient squared) algorithm proposed by Sonneveld [36], and CGSTAB (CGS stabilized) proposed by Van den Vorst [37]. In this work, the CGSTAB method [34] is used to solve the discretized equations, because it is stable and robust, easy to program, and has a fast convergence rate. Since the different directions are coupled by scattering term in equation (6), the discretized equations of radiative transfer are solved iteratively.

2.2. Inverse problem

For the inverse problem, the source term distribution is regarded as unknown, but the other quantities in equations (1) and (2) are known. In addition, some measured radiative intensities exiting boundaries are considered available. In the inverse analysis, the source term distribution is estimated by the measured data of exit radiative intensities.

The source term can be represented by a polynomial as

$$S(\boldsymbol{\tau})=\sum_{i=0}^{Q}\sum_{j=0}^{R}\sum_{k=0}^{S}c_{ijk}\,f_i(\xi)\,g_j(\eta)\,h_k(\zeta) \tag{12}$$

Here, f_i, g_j and h_k are basis functions as the polynomials $\{\xi^i\}$, $\{\eta^j\}$ and $\{\zeta^k\}$, respectively; c_{ijk} are the coefficients of the expansion. The inverse radiation problem can be formulated as an optimization problem. Usually, we wish to minimize the objective function

$$\Gamma\left(\boldsymbol{c}^k\right)=\sum_{i=1}^{N}\left\{\sum_{\boldsymbol{n}_{w_i}\cdot\boldsymbol{s}^m<0}w^m\left[I^m\left(\boldsymbol{\tau}_{w_i};\boldsymbol{c}^k\right)-Y^m(\boldsymbol{\tau}_{w_i})\right]^2\right\} \tag{13}$$

where $Y^m(\boldsymbol{\tau}_{w_i})$ are measured exit radiative intensities at the boundaries; N is the number of sensor locations; $I^m(\boldsymbol{\tau}_w;\boldsymbol{c})$ is the radiative intensities at boundaries for an estimated vector $\boldsymbol{c}=(c_{000},c_{100},\ldots,c_{\mathrm{QRS}})^{\mathrm{T}}$; QRS is the order of source term polynomial expansion. Thus, the inverse problem is reduced to an optimization problem in $(Q+1)(R+1)(S+1)$-dimensional space.

2.3. Conjugate gradient method of minimization

The minimization of the objective function with respect to the desired vector is the most important procedure in solving the inverse problem. In this paper, we use the conjugate gradient method to determine the unknown source term distribution of medium. Iterations are built in the following manner [38]:

$$\boldsymbol{c}^{k+1}=\boldsymbol{c}^k-\mu^k\boldsymbol{d}^k \tag{14}$$

where μ^k is the step size, $\boldsymbol{d}^k$ is the direction vector of descent given by

$$\boldsymbol{d}^k=\nabla\Gamma^{\mathrm{T}}\left(\boldsymbol{c}^k\right)+\nu^k\boldsymbol{d}^{k-1} \tag{15}$$

and the conjugate coefficient ν^k is determined from

$$\nu^k=\frac{\nabla\Gamma(\boldsymbol{c}^k)\nabla\Gamma^{\mathrm{T}}(\boldsymbol{c}^k)}{\nabla\Gamma(\boldsymbol{c}^{k-1})\nabla\Gamma^{\mathrm{T}}(\boldsymbol{c}^{k-1})}\quad\text{with }\nu^0=0 \tag{16}$$

Here, the row vector defined by

$$\nabla\Gamma=\left(\frac{\partial\Gamma}{\partial c_{000}},\frac{\partial\Gamma}{\partial c_{100}},\ldots,\frac{\partial\Gamma}{\partial c_{\mathrm{QRS}}}\right) \tag{17}$$

is the gradient of the objective function. Its components are defined as

$$\frac{\partial\Gamma(\boldsymbol{c}^k)}{\partial c_{ijk}}=2\sum_{l=1}^{N}\left\{\sum_{\boldsymbol{n}_{w_l}\cdot\boldsymbol{s}^m<0}w^m\left[I^m\left(\boldsymbol{\tau}_{w_l};\boldsymbol{c}^k\right)-Y^m(\boldsymbol{\tau}_{w_l})\right]\cdot\frac{\partial I^m(\boldsymbol{\tau}_{w_l};\boldsymbol{c}^k)}{\partial c_{ijk}}\right\} \tag{18}$$

In principle, the step size of the kth iteration, μ^k, can be determined by minimizing the function $\Gamma(\boldsymbol{c}-\mu^k\boldsymbol{d}^k)$ for the given $\boldsymbol{c}^k$ and $\boldsymbol{d}^k$ in the following manner:

$$\frac{\partial \Gamma(\boldsymbol{c}^k-\mu^k\boldsymbol{d}^k)}{\partial \mu^k}=0 \tag{19}$$

Since $\Gamma(\boldsymbol{c}^k-\mu^k\boldsymbol{d}^k)$ is the implicit function of $\mu^k\boldsymbol{d}^k$, the exact step size is difficult to be solved. As the first-order approximation, we make the first-order Taylor expansion of the function with respect to μ^k. Using equation (19), we have

$$\begin{aligned}\mu^k = &\left\{\sum_{l=1}^{N}\left\{\sum_{\boldsymbol{n}_{w_l}\cdot\boldsymbol{s}^m<0} w^m\left[I^m\left(\tau_{w_l};\boldsymbol{c}^k\right)-Y^m(\tau_{w_l})\right]\right.\right.\\ &\left.\left.\cdot\left[\nabla I^m\left(\tau_{w_l};\boldsymbol{c}^k\right)\cdot\boldsymbol{d}^k\right]\right\}\right\}\\ &\cdot\left\{\sum_{l=1}^{N}\left\{\sum_{\boldsymbol{n}_{w_l}\cdot\boldsymbol{s}^m<0} w^m\left[\nabla I^m\left(\tau_{w_l};\boldsymbol{c}^k\right)\cdot\boldsymbol{d}^k\right]^2\right\}\right\}^{-1}\end{aligned} \tag{20}$$

Here, the row vector

$$\nabla I^m=\left(\frac{\partial I^m}{\partial c_{000}},\frac{\partial I^m}{\partial c_{100}},\ldots,\frac{\partial I^m}{\partial c_{\mathrm{QRS}}}\right) \tag{21}$$

is the sensitivity coefficient vector. To perform the iteration given by equations (14)–(21), the sensitivity coefficient vector ∇I^m is required. In order to calculate ∇I^m, a sensitivity problem is developed as described below.

2.4. Sensitivity problem

To obtain the sensitivity coefficients, we substitute equation (12) into equations (5) and (6) and differentiate them with respect to c_{ijk}. The equation of sensitivity coefficients can be written as

$$\begin{aligned}&\frac{\partial}{\partial\xi}\left[\left(\alpha^m\xi_x+\beta^m\xi_y+\gamma^m\xi_z\right)J\frac{\partial I^m}{\partial c_{ijk}}\right]\\ &\quad+\frac{\partial}{\partial\eta}\left[\left(\alpha^m\eta_x+\beta^m\eta_y+\gamma^m\eta_z\right)J\frac{\partial I^m}{\partial c_{ijk}}\right]\\ &\quad+\frac{\partial}{\partial\zeta}\left[\left(\alpha^m\zeta_x+\beta^m\zeta_y+\gamma^m\zeta_z\right)J\frac{\partial I^m}{\partial c_{ijk}}\right]\\ &=J\left[-\frac{\partial I^m}{\partial c_{ijk}}+f_i(\xi)g_j(\eta)h_k(\zeta)\right.\\ &\qquad\left.+\frac{\omega_s}{4\pi}\sum_{m'=1}^{M}w^{m'}\Phi^{mm'}\frac{\partial I^{m'}}{\partial c_{ijk}}\right]\end{aligned} \tag{22}$$

with boundary conditions

$$\frac{\partial I^m(\boldsymbol{\tau}_w)}{\partial c_{ijk}}=0,\qquad \boldsymbol{n}_w\cdot\boldsymbol{s}^m>0 \tag{23}$$

In the same way as the discretization of direct problem, the final discretized equation for the sensitivity coefficients can be written as

$$\begin{aligned}a_{\mathrm{P}}^m\left[\frac{\partial I^m}{\partial c_{ijk}}\right]_{\mathrm{P}}=&a_{\mathrm{E}}^m\left[\frac{\partial I^m}{\partial c_{ijk}}\right]_{\mathrm{E}}+a_{\mathrm{W}}^m\left[\frac{\partial I^m}{\partial c_{ijk}}\right]_{\mathrm{W}}\\ &+a_{\mathrm{N}}^m\left[\frac{\partial I^m}{\partial c_{ijk}}\right]_{\mathrm{N}}+a_{\mathrm{S}}^m\left[\frac{\partial I^m}{\partial c_{ijk}}\right]_{\mathrm{S}}\\ &+a_{\mathrm{T}}^m\left[\frac{\partial I^m}{\partial c_{ijk}}\right]_{\mathrm{T}}+a_{\mathrm{B}}^m\left[\frac{\partial I^m}{\partial c_{ijk}}\right]_{\mathrm{B}}+b^m\end{aligned} \tag{24}$$

where the coefficients a are the same as given in equations (10a)–(10g), and

$$\begin{aligned}b^m=J_{\mathrm{P}}\Bigg[&f_i(\xi)g_j(\eta)h_k(\zeta)\\ &+\frac{\omega}{4\pi}\sum_{m'=1,m'\neq m}^{M}w^{m'}\Phi^{mm'}\frac{\partial I^{m'}}{\partial c_{ijk}}\Bigg]_{\mathrm{P}}\Delta\xi\Delta\eta\Delta\zeta\end{aligned} \tag{25}$$

A similar numerical iteration procedure as the direct problem is used for the solution of the discretized equation (24) of sensitivity problem, and will not be repeated here. Because the sensitivity coefficient vector ∇I is independent of the vector $\boldsymbol{c}$, the estimation of the source term distribution is linear.

2.5. Stopping criterion

The stopping criterion of iteration is selected in the following manner: if the problem contains no measurement errors, the following condition

$$\Gamma\left(\boldsymbol{c}^k\right)<\varepsilon \tag{26a}$$

is used for terminating the iterative process, otherwise, the condition

$$\Gamma\left(\boldsymbol{c}^k\right)<\sum_{i=1}^{N}\sum_{\boldsymbol{n}_{w_i}\cdot\boldsymbol{s}^m<0}w^m\left[\sigma_i^m\right]^2 \tag{26b}$$

is used as the stopping criterion. Here, ε is a small specified positive number, and σ_i^m is the standard deviation of the measurement errors.

2.6. Computational algorithm

The computational algorithm for the solution of the inverse radiation problem in this paper can be summarized as follows.

Step 1. Pick the initial guesses of $\boldsymbol{c}^0$. Set $k = 0$.

Step 2. Solve the sensitivity problem given by equations (22) and (23), and compute the sensitivity coefficient vector ∇I.

Step 3. Solve the direct problem given by equations (1) and (2), and compute the exit radiation intensities $I^m(\boldsymbol{\tau}; \boldsymbol{c}^k)$.

Step 4. Calculate objective function $\Gamma(\boldsymbol{c}^k)$ given by equation (13). Terminate the iteration process if the specified stopping criterion is satisfied. Otherwise, go to step 5.

Step 5. Compute the gradient $\nabla\Gamma(\boldsymbol{c}^k)$ from equation (18).

Step 6. Knowing $\nabla\Gamma(\boldsymbol{c}^k)$, compute the conjugate coefficient ν^k from equation (16), then compute the direction vector of descent $\boldsymbol{d}^k$ from equation (15).

Step 7. Knowing ∇I, $I^m(\boldsymbol{\tau}; \boldsymbol{c}^k)$, compute the step size μ^k from equation (20).

Step 8. Knowing μ^k and $\boldsymbol{d}^k$, compute the new estimated vector $\boldsymbol{c}^{k+1}$ from equation (14).

Step 9. Set $k = k + 1$, and go back to step 3.

To start the iteration, the initial guess $\boldsymbol{c}^0 = \boldsymbol{0}$ is used.

3. RESULTS AND DISCUSSION

Based on the theoretical and numerical analyses described earlier, a computer code has been developed to solve the inverse radiation problem of source term in general body-fitted coordinates. To examine the accuracy and computational efficiency of the method developed in this paper, an irregular geometric system is selected. The S_6 quadrature scheme was employed in the DOM. The schematic of the irregular geometric system and the body-fitted grid ($N_\xi \times N_\eta \times N_\zeta = 19 \times 19 \times 39$) are shown in *figure 1*. The top wall is located at $y = 2.0$, the left wall at $x = 0$, the right wall at $x = 2.0$, the front wall

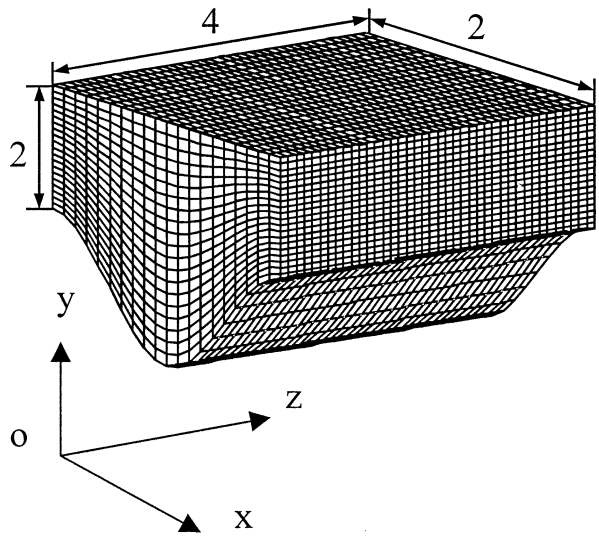

Figure 1. Schematic of the irregular geometric system and the body-fitted grid.

at $z = 0$, and rear wall at $z = 4.0$. The bottom wall varies according to the following function:

$$y = \cos(\pi x) - 1, \quad 0 \le x \le 2 \tag{27}$$

To examine the effectiveness of the method presented in this paper, three different test cases are considered. In the first case, the effects of measurement errors on the estimation of source term are considered. In the second case, it is assumed that the relating parameters, such as single scattering albedo and scattering phase function, have not errors, and the effects of them on the estimation of source term are examined. In the third, assuming that all of the relating parameters stated above have errors, we analyze the effects of these errors on the source term estimation.

To demonstrate the effects of measurement errors on the predicted source term, we consider the random errors. The simulated measured exit radiative intensities with random errors are obtained by adding normally distributed errors into the exact radiative intensities on the boundaries as

$$Y_{\text{measured}} = Y_{\text{exact}} + \sigma\varsigma \tag{28}$$

Here, ς is a normal distribution random variable with zero mean and unit standard deviation. The standard deviations of measured intensities, σ for a δ % measured error at 99 % confidence, are determined as

$$\sigma = \frac{Y_{\text{exact}} \cdot \delta\,\%}{2.576} \tag{29}$$

TABLE I
Sensor disposition and its position ($N = 6$).

Sensor No.	Sensor position	
	Boundary	(x, y, z)
1	left wall	(0.0, 1.0, 2.0)
2	right wall	(2.0, 1.0, 2.0)
3	bottom wall	(1.0, −2.0, 2.0)
4	top wall	(1.0, 2.0, 2.0)
5	front wall	(1.0, 0.0, 0.0)
6	rear wall	(1.0, 0.0, 4.0)

where 2.576 arises from the fact that 99 % of a normally distributed population is contained within ±2.576 standard deviation of the mean.

For the sake of comparison, maximum relative error E_{relm} and root mean square (RMS) error E_{rms} are defined as follows:

$$E_{\text{relm}} = \max\left\{\left|100\frac{S_{\text{estimated}}(\boldsymbol{\tau}) - S_{\text{exact}}(\boldsymbol{\tau})}{S_{\text{exact}}(\boldsymbol{\tau})}\right|\right\} \quad (30)$$

$$E_{\text{rms}} = \left\{\frac{1}{V}\iiint_V \left[S_{\text{estimated}}(\boldsymbol{\tau}) - S_{\text{exact}}(\boldsymbol{\tau})\right]^2 \cdot J\,\mathrm{d}\xi\,\mathrm{d}\eta\,\mathrm{d}\zeta\right\}^{0.5} \quad (31)$$

In the following conclusion, we consider a source term distribution represented as

$$S(\boldsymbol{\tau}) = 80 + 200\xi + 160\eta + 40\zeta - 100\xi^2 - 80\eta^2 - 10\zeta^2\ [\mathrm{W{\cdot}m^{-2}{\cdot}sr^{-1}}] \quad (32)$$

The average value of the source term, S_{av}, is 231.94 $\mathrm{W{\cdot}m^{-2}{\cdot}sr^{-1}}$. The scattering phase function of media is assumed to be linear anisotropic, given as

$$\Phi\left(\boldsymbol{s}^m, \boldsymbol{s}^{m'}\right) = 1 + g\left(\alpha^m\alpha^{m'} + \beta^m\beta^{m'} + \gamma^m\gamma^{m'}\right) \quad (33)$$

Here, g is the scattering asymmetry parameter.

3.1. Case A

We considered two sets of sensor disposition scheme as given in *tables I* and *II*. In the first set, the number of sensors used to measure exit radiative intensity data N is 6, and in the second set, N is 24. With no measurement errors, the errors of source term are $E_{\text{rms}} = 0.027$ and $E_{\text{relm}} = 0.065\,\%$ for 6 sensors, and $E_{\text{rms}} = 0.015$ and $E_{\text{relm}} = 0.034\,\%$ for 24 sensors. The agreement between the estimated and the exact values of the source term is excellent. Simulated experimental data containing random measurement errors of $\delta = 2\,\%$ and $5\,\%$ are used to estimate the source term with inverse analysis. The results of 20 samples are shown in *figures 2* and *3*. Clearly, increasing δ from 2 to 5 %, the accuracy of the estimation decreases, and increasing the number of sensors N from 6 to 24, the accuracy of the estimation is improved obviously. Because the measured exit radiative intensities are available only at the positions far from the corners, the errors of the estimation are larger near the corners. Even in the case of $\delta = 5\,\%$ and $N = 6$, the maximum value of the ratio $E_{\text{rms}}/S_{\text{av}}$ is less than 0.04, the estimation of the source term is good.

TABLE II
Sensor disposition and its position ($N = 24$).

Sensor No.	Sensor position	
	Boundary	(x, y, z)
1	left wall	(0.0, 1.0, 0.97)
2	left wall	(0.0, 1.0, 3.03)
3	left wall	(0.0, 0.47, 2.0)
4	left wall	(0.0, 1.53, 2.0)
5	right wall	(2.0, 1.0, 0.97)
6	right wall	(2.0, 1.0, 3.03)
7	right wall	(2.0, 0.47, 2.0)
8	right wall	(2.0, 1.53, 2.0)
9	bottom wall	(1.0, −2.0, 0.97)
10	bottom wall	(1.0, −2.0, 3.03)
11	bottom wall	(0.47, −0.91, 2.0)
12	bottom wall	(1.53, −0.91, 2.0)
13	top wall	(1.0, 2.0, 0.97)
14	top wall	(1.0, 2.0, 3.03)
15	top wall	(0.47, 2.0, 2.0)
16	top wall	(1.53, 2.0, 2.0)
17	front wall	(1.0, −1.05, 0.0)
18	front wall	(1.0, 1.05, 0.0)
19	front wall	(0.47, 0.0, 0.0)
20	front wall	(1.53, 0.0, 0.0)
21	rear wall	(1.0, −1.05, 4.0)
22	rear wall	(1.0, 1.05, 4.0)
23	rear wall	(0.47, 0.0, 4.0)
24	rear wall	(1.53, 0.0, 4.0)

3.2. Case B

We now separately examine the effects of the single scattering albedo and scattering asymmetry parameter on the accuracy of the inverse estimation. It is assumed that the relating parameters stated above have no errors, and the measured exit radiative intensities are of no measurement error. The effects of single scattering albedo on the

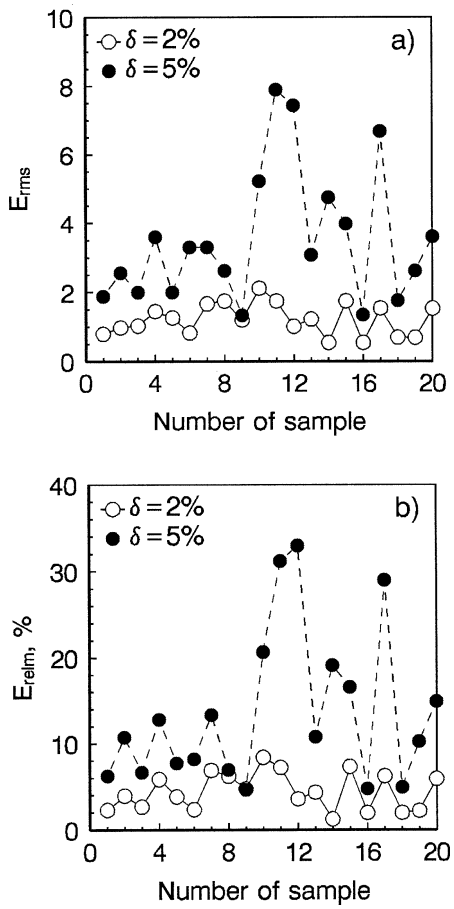

Figure 2. Errors of the source term estimation with inverse analysis for the case $N = 6$, $\omega = 0.5$, $g = 0.0$ using simulated measured exit radiative intensity data with $\delta = 2\%$ and 5%: (a) RMS errors; (b) maximum relative errors.

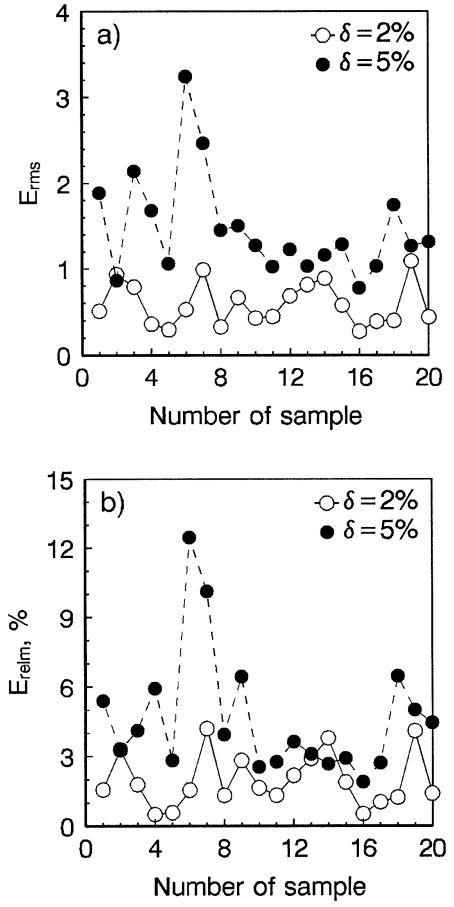

Figure 3. Errors of the source term estimation with inverse analysis for the case $N = 24$, $\omega = 0.5$, $g = 0.0$ using simulated measured exit radiative intensity data with $\delta = 2\%$ and 5%: (a) RMS errors; (b) maximum relative errors.

estimation of the source term are shown in *figure 4*. As shown in *figure 4*, within the range from $\omega = 0.1$ to 0.9, the effects of single scattering albedo are very small. To show the effects of anisotropic scattering on the source term estimation, forward scattering and backward scattering are considered. The effects of scattering asymmetry parameter on the estimation of the source term are shown in *figure 5*. All of the RMS errors are less than 0.05, and the maximum relative error is less than 0.2%. The effects of scattering asymmetry parameter on the estimation are not significant, and the results obtained with the inverse analysis are good.

3.3. Case C

In the practical processes of measurement and inverse solution, the parameters, such as the single scattering albedo and scattering asymmetry parameter, may have random errors more or less. The errors of these parameters and the measurement errors of exit radiative intensities often exist simultaneously. In order to examine the combined effects of these errors on source term estimation, it is assumed that single scattering albedo and scattering asymmetry parameter have normally distributed random errors and the random samples are generated by the following manner

$$\omega = \omega_{\text{exact}} + \sigma_\omega \varsigma \tag{34}$$

$$g = g_{\text{exact}} + \sigma_g \varsigma \tag{35}$$

The standard deviations, σ_ω and σ_g, are chosen as

$$\sigma_\omega = \frac{\omega_{\text{exact}} \cdot \rho_\omega \%}{2.576} \tag{36}$$

$$\sigma_g = \frac{g_{\text{exact}} \cdot \rho_g \%}{2.576} \tag{37}$$

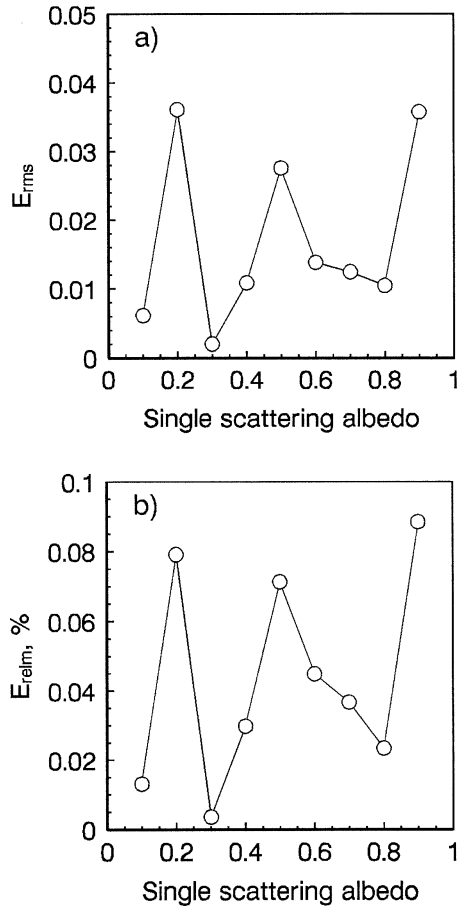

Figure 4. Effects of the single scattering albedo on the source term estimation for the case $N = 6$, $g = 0.0$: (a) RMS errors; (b) maximum relative errors.

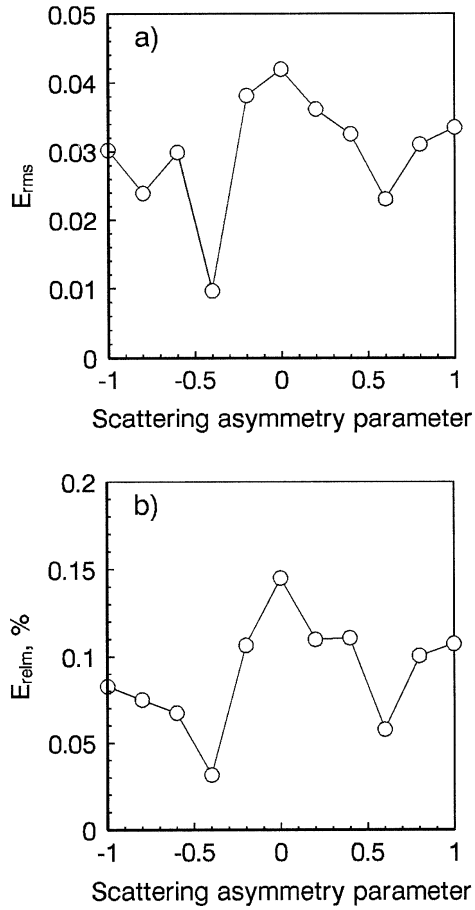

Figure 5. Effects of the scattering asymmetry parameter on the source term estimation for the case $N = 6$, $\omega = 0.5$: (a) RMS errors; (b) maximum relative errors.

Figure 6 shows the errors of the source term estimation for $\delta = \rho_\omega = \rho_g = 2\%$ and $N = 6$. In the 20 random samples, all of the RMS errors are less than 2.4, and the ratio $E_{\rm rms}/S_{\rm av}$ is less than 0.01. It can be seen that, even with noisy input data, the reconstruction of the source term is good. Comparing *figures 2* and *6*, we note that the errors of the source term estimation are mainly brought about by measurement errors of the exit radiative intensities. In order to improve the accuracy of the reconstruction of the source term, the measurement errors of the exit radiative intensities must be limited within an appropriate extent.

4. CONCLUSIONS

A method is presented to identify the three-dimensional source term distribution in complicated geometric systems of known radiative properties from the knowledge of the exit radiative intensities at boundaries. The inverse radiation problem is formulated as an optimization problem, and solved by the conjugate gradient method that minimizes the errors between the exit radiative intensities calculated and the experimental measurements. In this approach, the discrete ordinates method is employed to solve the direct and the sensitivity problems in general body-fitted coordinates. Although the source term is a function of space variables, only the measurements of exit radiative intensities at boundaries are required. Both exact and noisy input data have been used to test the performance of the proposed method. The results of this study show that the three-dimensional source term distribution in complicated geometric systems can be estimated accurately, even with noisy data.

The errors of the source term estimation are mainly brought about by measurement errors of the exit radiative

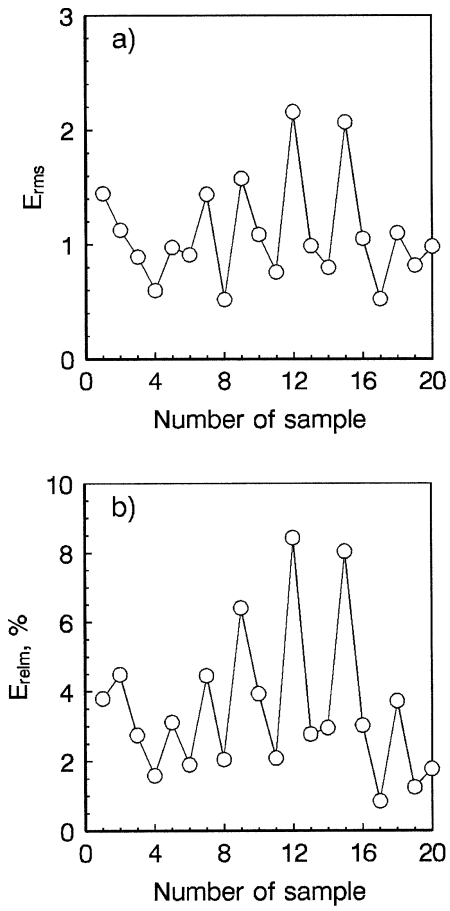

Figure 6. Errors of the source term estimation with inverse analysis for the case $N = 6$, $\omega_{exact} = 0.5$, $g_{exact} = 0.5$, using simulated measured exit radiative intensity data with $\delta = \rho_\omega = \rho_g = 2\%$: (a) RMS errors; (b) maximum relative errors.

intensities. In order to improve the accuracy of the reconstruction of the source term, the measurement errors of the exit radiative intensities must be confined to an appropriate limit. Increasing the number of sensors, the accuracy of the estimation can be improved.

Acknowledgements

The support of this work by the National Science Foundation of China, the Chinese National Science Fund for Distinguished Young Scholar, and the Fok Ying Tung Education Foundation is gratefully acknowledged.

REFERENCES

[1] McCormick N.J., A critique of inverse solutions to slab geometry transport problems, Progress in Nuclear Energy 8 (1981) 235–245.

[2] McCormick N.J., Recent developments in inverse scattering transport method, Transport Theory and Statistical Physics 13 (1984) 15–28.

[3] McCormick N.J., Methods for solving inverse problems for radiation transport — an update, Transport Theory and Statistical Physics 15 (1986) 759–772.

[4] McCormick N.J., Inverse radiative transfer problems: A review, Nuclear Science and Engineering 112 (1992) 185–198.

[5] Sanchez R., McCormick N.J., Numerical evaluation of optical single-scattering inverse transport methods, J. Quant. Spectrosc. Radiative Transfer 28 (1982) 169–184.

[6] Dunn W.L., Inverse Monte Carlo solutions for radiative transfer in inhomogeneous media, J. Quant. Spectrosc. Radiative Transfer 29 (1983) 19–26.

[7] Kamiuto K., Seki J., Study of the P_1 approximation in an inverse scattering problem, J. Quant. Spectrosc. Radiative Transfer 37 (1987) 455–459.

[8] Ho C.H., Ozisik M.N., An inverse radiation problem, Int. J. Heat Mass Tran. 32 (1989) 335–341.

[9] Subramaniam S., Menguc M.P., Solution of the inverse radiation problem for inhomogeneous and anisotropically scattering media using a Monte Carlo technique, Int. J. Heat Mass Tran. 34 (1991) 253–266.

[10] Kamiuto K., Iwanmoto M., Nishimura T., Albedo and asymmetry factors of the phase functions for packed-sphere systems, J. Quant. Spectrosc. Radiative Transfer 46 (1991) 309–316.

[11] Kamiuto K., Emerging-flux fitting method for inverse scattering problems, J. Quant. Spectrosc. Radiative Transfer 49 (1993) 263–267.

[12] Menguc M.P., Manickavasagam S., Inverse radiation problem in axisymmetric cylindrical scattering media, J. Thermophys. Heat Tran. 7 (1993) 479–486.

[13] Ligon D.A., Chen T.W., Gillespie J.B., Determination of aerosol parameters from light-scattering data using an inverse Monte Carlo technique, Applied Optics 35 (1996) 4297–4303.

[14] Neto A.J.S., Ozisik M.N., An inverse problem of simultaneous estimation of radiation phase function, albedo and optical thickness, J. Quant. Spectrosc. Radiative Transfer 53 (1995) 397–409.

[15] Barichello L.B., Garcia R.D.M., Siewert C.E., On inverse boundary-condition problems in radiative transfer, J. Quant. Spectrosc. Radiative Transfer 57 (1997) 405–410.

[16] Henry J.F., Bissieux C., Marquie S., One-dimensional modeling and parameter estimation in scattering media, High Temp. High Press. 29 (1997) 159–164.

[17] Yi H.C., Sanchez R., McCormick N.J., Bioluminescence estimation from ocean in situ irradiances, Applied Optics 31 (1992) 822–830.

[18] Li H.Y., Ozisik M.N., Identification of the temperature profile in an absorbing, emitting, and isotropically scattering medium by inverse analysis, J. Heat Tran. 114 (1992) 1060–1063.

[19] Li H.Y., Ozisik M.N., Inverse radiation problem for simultaneous estimation of temperature profile and surface reflectivity, J. Thermophys. Heat Tran. 7 (1993) 88–93.

[20] Siewert C.E., A new approach to the inverse problem, J. Math. Phys. 19 (1978) 2619–2621.

[21] Siewert C.E., An inverse source problem in radiative transfer, J. Quant. Spectrosc. Radiative Transfer 50 (1993) 603–609.

[22] Siewert C.E., A radiative-transfer inverse-source problem for a sphere, J. Quant. Spectrosc. Radiative Transfer 52 (1994) 157–160.

[23] Li H.Y., Estimation of the temperature profile in a cylindrical medium by inverse analysis, J. Quant. Spectrosc. Radiative Transfer 52 (1994) 755–764.

[24] Li H.Y., An inverse source problem in radiative transfer for spherical media, Numer. Heat Tran. Part B 31 (1997) 251–260.

[25] Liu L.H., Tan H.P., Yu Q.Z., Inverse radiation problem of boundary incident radiation heat flux in semitransparent planar slab with semitransparent boundaries, J. Therm. Sci. 7 (1998) 131–138.

[26] Liu L.H., Tan H.P., Yu Q.Z., Inverse radiation problem in one-dimensional semitransparent plane-parallel media with opaque and specularly reflecting boundaries, J. Quant. Spectrosc. Radiative Transfer 64 (2000) 395–407.

[27] Liu L.H., Tan H.P., Yu Q.Z., Simultaneous identification of temperature profile and wall emissivities in semitransparent medium by inverse radiation analysis, Numer. Heat Tran. Part A 36 (1999) 511–525.

[28] Li H.Y., Inverse radiation problem in two-dimensional rectangular media, J. Thermophys. Heat Tran. 11 (1997) 556–561.

[29] Liu L.H., Tan H.P., Yu Q.Z., Inverse radiation problem of temperature field in three-dimensional rectangular furnaces, Int. Comm. Heat Mass Tran. 26 (1999) 239–248.

[30] Modest M.F., Radiative Heat Transfer, McGraw-Hill, New York, 1993.

[31] Fiveland W.A., Discrete ordinate methods for radiative heat transfer in isotropically and anisotropically media, J. Heat Tran. 109 (1987) 809–812.

[32] Truelove J.S., Three-dimensional radiation in absorbing-emitting-scattering media using the discrete ordinates approximation, J. Quant. Spectrosc. Radiative Transfer 39 (1988) 27–31.

[33] Jamaluddin A.S., Smith P.J., Discrete-ordinates solution of radiative transfer equation in nonaxisymmetric cylindrical enclosures, J. Thermophys. Heat Tran. 6 (1992) 242–245.

[34] Ferziger J.H., Peric M., Computational Methods for Fluid Dynamics, Springer-Verlag, Berlin, 1997.

[35] Liu J., Shang H.M., Chen Y.S., Prediction of radiative transfer in general body-fitted coordinates, Numer. Heat Tran. Part B 31 (1997) 423–439.

[36] Sonneveld P., CGS: a fast Lanczos type solver for non-symmetric liner systems, SIAM J. Sci. Stat. Comput. 10 (1989) 36–52.

[37] Van den Vorst H.A., BI-CGSTAB: a fast and smoothly converging variant of BI-CG for the solution of non-symmetric linear systems, SIAM J. Sci. Stat. Comput. 13 (1992) 631–644.

[38] Yuan Y.X., Sun W.Y., Optimization Theory and Methods, Science Press, Beijing, 1997.